Comparative Proteomics Indicates That Biosynthesis of Pectic Precursors Is Important for Cotton Fiber and *Arabidopsis* Root Hair Elongation*[S]

Chao-You Pang‡§¶, Hui Wang‡¶, Yu Pang‡, Chao Xu‡, Yue Jiao‡, Yong-Mei Qin‡, Tamara L. Western‖, Shu-Xun Yu¶§, and Yu-Xian Zhu‡ ‡‡§§¶¶**

The quality of cotton fiber is determined by its final length and strength, which is a function of primary and secondary cell wall deposition. Using a comparative proteomics approach, we identified 104 proteins from cotton ovules 10 days postanthesis with 93 preferentially accumulated in the wild type and 11 accumulated in the *fuzzless-lintless* mutant. Bioinformatics analysis indicated that nucleotide sugar metabolism was the most significantly upregulated biochemical process during fiber elongation. Seven protein spots potentially involved in pectic cell wall polysaccharide biosynthesis were specifically accumulated in wild-type samples at both the protein and transcript levels. Protein and mRNA expression of these genes increased when either ethylene or lignoceric acid (C24:0) was added to the culture medium, suggesting that these compounds may promote fiber elongation by modulating the production of cell wall polymers. Quantitative analysis revealed that fiber primary cell walls contained significantly higher amounts of pectin, whereas more hemicellulose was found in ovule samples. Significant fiber growth was observed when UDP-L-rhamnose, UDP-D-galacturonic acid, or UDP-D-glucuronic acid, all of which were readily incorporated into the pectin fraction of cell wall preparations, was added to the ovule culture medium. The short root hairs of *Arabidopsis uer1-1* and *gae6-1* mutants were complemented either by genetic transformation of the respective cotton cDNA or by adding a specific pectin precursor to the growth medium. When two pectin precursors, produced by either UDP-4-keto-6-deoxy-D-glucose 3,5-epimerase 4-reductase or by UDP-D-glucose dehydrogenase and UDP-D-glucuronic acid 4-epimerase successively, were used in the chemical complementation assay, wild-type root hair lengths were observed in both *cut1* and *ein2-5 Arabidopsis* seedlings, which showed defects in C24:0 biosynthesis or ethylene signaling, respectively. Our results suggest that ethylene and C24:0 may promote cotton fiber and *Arabidopsis* root hair growth by activating the pectin biosynthesis network, especially UDP-L-rhamnose and UDP-D-galacturonic acid synthesis. *Molecular & Cellular Proteomics 9:2019–2033, 2010.*

Cell elongation and expansion contribute significantly to the growth and morphogenesis of higher plants. Cotton (*Gossypium hirsutum*) fibers are single cells that differentiate from the outer integuments of the ovule. Cotton lint (the industrial name for fiber) is the most prevalent natural raw material used in the textile industry, so its production plays a significant role in the global economy. The number of fibers present on each ovule (cotton productivity), the final length, and the strength of each fiber (fiber quality) are determined by four separable biological processes: fiber initiation, elongation (primary cell wall synthesis), cell wall thickening (secondary cell wall deposition), and maturation. The fiber initiation stage occurs from 3 days prior to anthesis to 3 days postanthesis (dpa)[1] and is characterized by the enlargement and protrusion of epidermal cells from the ovule surface. During the fiber elongation period (5–25 dpa), cells demonstrate vigorous expansion with peak growth rates of >2 mm/day until the fibers reach their final dimensions (1–3). In the secondary cell wall deposition phase (20–45 dpa), cellulose biosynthesis predominates until the cells

From the ‡The National Laboratory of Protein Engineering and Plant Genetic Engineering and §§Peking-Yale Joint Center for Plant Molecular Genetics and Agrobiotechnology, College of Life Sciences, Peking University, Beijing 100871, China, §Cotton Research Institute, Chinese Academy of Agricultural Sciences, Anyang 455000, Henan Province, China, ‖Department of Biology, McGill University, 1205 Avenue Docteur Penfield, Montreal, Quebec H3A 1B1, Canada, and ‡‡National Center for Plant Gene Research, Beijing 100101, China

Received, May 7, 2010, and in revised form, June 4, 2010

Published, MCP Papers in Press, June 6, 2010, DOI 10.1074/mcp.M110.000349

[1] The abbreviations used are: dpa, days postanthesis; UER, UDP-4-keto-6-deoxy-D-glucose 3,5-epimerase 4-reductase; UGP, UDP-D-glucose pyrophosphorylase; UGD, UDP-D-glucose dehydrogenase; GAE, UDP-D-glucuronic acid 4-epimerase; Rha, L-rhamnose; Xyl, D-xylose; GalA, D-galacturonic acid; GlcA, D-glucuronic acid; 2-DE, two-dimensional gel electrophoresis; fl, fuzzless-lintless; S/N, signal to noise ratio; RACE, rapid amplification of 5′ or 3′ cDNA ends; BLAST, basic local alignment search tool; FDR, false discovery rate; QRT-PCR, quantitative real time RT-PCR; At, *Arabidopsis thaliana*; Gh, *G. hirsutum*; 4K6DG, 4-keto-6-deoxyglucose; AVG, L-(2-aminoethoxyvinyl)glycine hydrochloride; KEGG, Kyoto Encyclopedia of Genes and Genomes; RHM, rhamnose synthase; NCBI, National Center for Biotechnology Information; UGE, UDP-glucose 4-epimerase.

contain ~90% cellulose. In the final maturation stage (45–50 dpa), fibers undergo dehydration and become mature cotton lint.

Cotton fibers also serve as an excellent single celled model for studying fundamental biological processes, including cell elongation and differentiation (4–6). Using cDNA microarray hybridization data obtained from 11,692 cotton fiber UniESTs, we previously identified 778 cDNAs that are preferentially expressed during the fast fiber elongation period (7). Among them, 162 fiber-preferential genes were mapped to 102 metabolic events with ethylene biosynthesis and fatty acid biosynthesis/chain elongation being the most significantly up-regulated processes. Systematic studies showed that a large number of genes encoding nonspecific lipid transfer proteins and enzymes that are involved in various steps of fatty acid chain elongation are highly up-regulated during early fiber development, indicating that biosynthesis of saturated very-long-chain fatty acids and/or their transport may also be required for fiber cell growth (3, 7–11). Exogenously applied lignoceric acid (C24:0) in the ovule culture medium promotes significant fiber cell growth, possibly by activating the transcription of several 1-aminocyclopropane-1-carboxylic acid oxidases involved in ethylene biosynthesis (12). To date, biochemical reactions downstream of ethylene signaling that lead to cell elongation have not been reported.

Two-dimensional gel electrophoresis (2-DE) coupled with MALDI-TOF MS has recently been used to study brassinosteroid signal transduction pathways (13) and to decipher complex metabolomics data obtained from abiotic stresses in *Arabidopsis* and in rice (14, 15). Here we found that the biosynthesis of a specific subset of carbohydrates, including UDP-Rha, UDP-GlcA, and UDP-GalA, required for pectic polymer production, was significantly activated in developing fiber cells. Genetic studies using a series of *Arabidopsis* mutants with defects in UDP-Rha and UDP-GalA biosynthesis or in control of upstream regulatory components confirmed the importance of these two metabolic steps for both cotton fiber and *Arabidopsis* root hair growth.

EXPERIMENTAL PROCEDURES

Plant Materials—Upland cotton (*G. hirsutum* L. cv. Xuzhou 142) and the *fuzzless-lintless* (*fl*) mutant, originally discovered in the Xuzhou 142 cotton field in China (16), were grown in an artificial soil mixture in fully climate-controlled walk-in growth chambers. Bolls excised from cotton plants at the indicated growth stages were dissected in a laminar flow hood to obtain intact ovules. Cotton materials were frozen and stored in liquid nitrogen immediately after harvest until use for protein and RNA extractions. All *Arabidopsis* plants, including three mutant lines in the Col genetic background (*ein2-5*; At *uer1-1*, SALK_100812; At *gae6-1*, SALK_104454C) and the *cut1* mutant in the Ler genetic background, were grown in fully automated growth chambers as described (17).

Protein Extraction and Purification—Plant tissues were ground in liquid nitrogen using a mortar and pestle. Fine powder was produced at −20 °C with 10% (w/v) trichloroacetic acid in cold acetone containing 0.07% (w/v) 2-mercaptoethanol for at least 2 h. After centrifugation at 20,000 × *g* for 1 h, the pellet was washed first with cold acetone containing 0.07% (w/v) 2-mercaptoethanol and then with 80% cold acetone and finally suspended in a lysis buffer (7 M urea, 2 M thiourea, 4% CHAPS, 20 mM dithiothreitol), and the soluble fraction was purified using the 2-D Clean-Up kit (GE Healthcare). Protein concentration was determined with a 2-D Quant kit (GE Healthcare).

Two-dimensional Gel Electrophoresis—2-DE was performed as described (18, 19). Total cotton ovule proteins (100 μg or 1.5 mg) were applied for silver- or Coomassie-stained gels, respectively. Isoelectric focusing was performed with the IPGphor system (GE Healthcare). Immobiline pH 4–7 and 3–10, 24-cm linear DryStrips (GE Healthcare) were run at 30 V for 8 h, 50 V for 4 h, 100 V for 1 h, 300 V for 1 h, 500 V for 1 h, 1000 V for 1 h, and 8000 V for 12 h using rehydration buffer (8 M urea, 2% CHAPS, 20 mM DTT) containing 0.5% (v/v) IPG Buffer (GE Healthcare). SDS-PAGE was performed using 12.5% polyacrylamide gels without a stacking gel in the Ettan Dalt*six* Electrophoresis Unit 230 (GE Healthcare). Gels were stained with 0.04% (w/v) PhastGel Blue R (Coomassie Brilliant Blue R-350; GE Healthcare) in 10% acetic acid and destained with 10% acetic acid or were silver-stained using a Hoefer Automated Gel Stainer apparatus. Images of the gels were scanned by a PowerLook 2100XL (UMAX) and analyzed using ImageMaster 2-DE Elite (version 4.01, Amersham Biosciences). Protein samples were prepared in triplicate using different plant materials for each 2-DE image.

Protein Identification by MALDI-TOF/TOF MS—Differentially expressed proteins were excised and digested with trypsin essentially as reported (20). Mass spectra were recorded on an Ultraflex MALDI-TOF/TOF mass spectrometer (Bruker Daltonik GmbH) using the FlexControl 2.2 software (Bruker Daltonik GmbH). TOF results were analyzed by FlexAnalysis 2.2 (Bruker Daltonik GmbH), peaks with S/N >100 were selected as precursor ions that were accelerated in TOF1 at a voltage of 8 kV and fragmented by lifting the voltage to 19 kV. Both MALDI-TOF and MS/MS spectra were processed by FlexAnalysis 2.2 (Bruker Daltonik GmbH) and were searched using MASCOT 2.1.0 (Matrix Science). All spectra were searched against the in-house National Center for Biotechnology Information non-redundant (NCBInr) database (release date, June 10, 2008; including 6,573,034 sequences, 2,244,863,856 residues) with species restriction to Viridiplantae (green plants) (483,288 sequences) and a cotton EST database downloaded from NCBI "EST others" (release date, January 22, 2009; including 369,596 sequences, 254,288,404 residues) ($p < 0.05$). We used the following parameters for the search: S/N ≥ 3.0; fixed modification, carbamidomethyl (Cys); variable modification, oxidation (Met); maximum number of missing cleavages, 1; MS tolerance, ±100 ppm; and MS/MS tolerance, ±0.7 Da. The ion cutoff score was 51 ($p < 0.01$, $E < 0.01$) following a published protocol (21).

Protein Identification by Nano-LC-FTICR MS—Several identified protein spots deemed potentially important were further analyzed using nano-liquid chromatography-Fourier transform ion cyclotron resonance-mass spectrometry (nano-LC-FTICR MS) techniques as described (22). Trypsin-digested peptides were dissolved in 0.1% formic acid and separated by a nano-LC system (Micro-Tech Scientific) that was equipped with a C_{18} reverse-phase column using 0–50% acetonitrile gradient in 0.1% formic acid at a constant flow rate of 400 nl/min in 120 min. Mass spectra were recorded on a 7-tesla FTICR mass spectrometer (Apex-Qe, Bruker Daltonics). Data were acquired in data-dependent mode using ApexControl 1.0 software (Bruker Daltonics). The MS/MS spectra were processed by DataAnalysis 3.4 (Bruker Daltonics) with S/N ≥4.0 and searched against the in-house cotton EST database using the Mascot 2.1.0 search engine (Matrix Science). Fixed and variable modifications were specified as described under "Protein Identification by MALDI-TOF/TOF MS." Maximum number of missing cleavages was set to 1. MS tolerance was ±5 ppm, and MS/MS tolerance was ±15 millimass units. The ion cutoff score was 41 ($p < 0.01$, $E < 0.01$). The criteria for

positive identification we used result in less than 5% false positives at the protein level as determined by searching a target-decoy database constructed with shuffled sequences in the decoy. The false-positive rate was calculated as follows: 2 × decoy hits/total hits (23).

Analysis of Full-length Cotton cDNAs—To obtain putative full-length cotton cDNAs, all 375,441 cotton ESTs available from NCBI (http://www.ncbi.nlm.nih.gov/Genbank/) as of April 10, 2009 were downloaded. Putative full-length cDNA sequences were obtained on a Linux operating system using the local cotton EST database, the BLAST results, and the CAP3 sequence assembly program (24). When a putative full-length cDNA was not available in our cDNA collection, we used rapid amplification of 5′ or 3′ cDNA ends (RACE) (17) to recover the missing sequences. The entire coding region with any available upstream and downstream sequences was amplified again to confirm that the RACE products were assembled correctly from a single gene and not from a chimeric gene sequence of the A and D subgenomes. All full-length cDNAs were verified by sequencing the corresponding clone from a cotton cDNA library that was constructed using RNA extracted with the hot borate method (25). We used guanidine hydrochloride (final concentration, 6 M) as the denaturant and 1% polyvinylpyrrolidone to remove major phenolic compounds from cotton ovule or fiber cells. The quality of the library was verified because putative open reading frames were found in more than half of the genes related to plant hormone biosynthesis (7).

Identification of Fiber-preferential Biochemical Pathways—The software KOBAS, which stands for Kyoto Encyclopedia of Genes and Genomes (KEGG) Orthology-based Annotation System (26), was used to identify biochemical reactions involved in cotton fiber development and to calculate the statistical significance of each step. This program assigns a given set of genes to pathways by first matching the genes to similar genes (as determined by a BLAST similarity search with cutoff E values $<1 \times 10^{-6}$, rank <5, and sequence identity $>55\%$) in known pathways in the KEGG database. We ranked pathways (or biochemical events) by statistical significance to determine whether a pathway contained a higher ratio of fiber-preferential proteins among all *Arabidopsis* proteins mapped to the same pathway. Because a large number of pathways were involved, we implemented FDR correction to control the overall Type I error rate of multiple testing using GeneTS (2.8.0) in the R (2.2.0) statistics software package. Pathways with FDR-corrected p values <0.001 were considered statistically significant.

RT-PCR and Quantitative Real Time RT-PCR (QRT-PCR)—Cotton ovules harvested at specific growth stages were first frozen in liquid nitrogen before RNA extraction using a modified hot borate method (25). Total RNA was extracted from wild-type or *fl* mutant cotton materials after various treatments, and cDNA was reverse transcribed from 5 μg of total RNA. Primers for QRT-PCR analysis are listed in supplemental Table 1. All PCR experiments were performed in triplicate using independent RNA samples prepared from different cotton or *Arabidopsis* materials. Cotton *UBQ7* (NCBI accession number AY189972) and *Arabidopsis UBQ5* (At3g62250) were used as internal controls for PCR experiments using the respective plant materials.

Preparation of Antiserum against UER1 and Western Blotting—Gh UER1-specific antibody was produced from rabbit using a synthesized polypeptide, KESLIKYVFEPNKKT, derived from the C terminus of UER1, which was identified commercially using Peptide-Antigen Finder software (Chinese Peptide Corp.). Western blotting experiments were performed as reported previously (27).

Extraction, Separation, and Analysis of Cell Wall Polymer Fractions—Either 10-dpa cotton fiber cells or ovules (5-g fresh weight) were ground in liquid nitrogen using a mortar and pestle. The fine powders were washed with 70% aqueous ethanol and pelleted by centrifugation at 10,000 × *g* for 15 min. The resulting pellet was washed with a 1:1 (v/v) mixture of chloroform and methanol and was then washed twice with acetone before drying in a SpeedVac vacuum system (Savant Instruments). Starch contaminants were removed by successive treatments with α-amylase (5 units/mg of cell wall; overnight at room temperature) (Sigma-Aldrich) and dimethyl sulfoxide (1 ml/mg of cell wall; overnight at room temperature). Pectin fractions were obtained by first boiling the cell wall pellets three times in 50 mM EDTA (pH 6.8; 10 min each) and then extracting three times at room temperature for 12 h in 50 mM Na_2CO_3 containing 1% $NaBH_4$. Hemicelluloses were successively extracted from remnant cell wall pellets in 1 M (three times) and 4 M (three times) KOH containing 1% $NaBH_4$ at room temperature for 12 h each time. The alkali fractions were neutralized with acetic acid. All six pectin and hemicellulose extracts were combined respectively and dialyzed extensively in dialysis tubing (1000-Da cutoff) against water. Both fractions were then concentrated using a Stirred Ultrafiltration Cell (Millipore) equipped with ultrafiltration membranes (1000-Da limit; Millipore), lyophilized to dryness, and weighed. The Updegraff assay (28) was used to determine relative cellulose content in the remaining cell wall pellets to deduce the amount of "other unidentified cell wall components" (called "others").

Analysis of Cell Wall Monosaccharide Composition—Starch-free total cell wall materials, purified pectin, and hemicellulose were subjected to 2 M TFA at 120 °C for 2 h to produce monosaccharides. The neutral monosaccharides were converted into alditol acetates, whereas uronic acids were derivatized by trimethylsilyl methoxime before GC/MS analysis (29, 30). Briefly, different fractions were run on a GC/MS instrument (6890N-5975B, Agilent Technologies) with helium as the carrier gas to determine their sugar composition. For alditol acetate derivatives, a J&W HP-5MS column (30 m × 0.25 mm × 0.25 μm; Agilent Technologies) was used with the following program: 2 min at 110 °C, 10 °C/min until 200 °C, 5 min at 200 °C, 10 °C/min until 250 °C, and hold at 250 °C for 10 min. For trimethylsilyl methoxime derivatives, a J&W DB-5MS column (30 m × 0.25 mm × 0.25 μm; Agilent Technologies) was used with the following program: 1 min at 160 °C, 10 °C/min until 172 °C, 5 °C/min to 208 °C, decrease to 200 °C in 10 s, hold at 200 °C for 2 min, decrease to 160 °C in 30 s, and hold at 160 °C for 2 min. Compounds were first confirmed by comparison with the retention time obtained from the individual monosaccharide standard and were further identified through GC/MS coupled to the National Institute of Standards and Technology (NIST) database.

In Vitro Expression and Purification of Enzymes—Putative full-length cotton *UER1*, *UGD1*, *UGP1*, *UGP2*, and *GAE3* cDNAs were cloned into pET28a to produce pET28a-GhUER1, pET28a-GhUGD1, pET28a-GhUGP1, pET28a-GhUGP2, and pET28a-GhGAE3, respectively. The plasmids were separately transformed into *Escherichia coli* BL21 (DE3) pLysS cells and were cultured at 37 °C with vigorous shaking in liquid LB medium containing 50 μg/ml kanamycin. Isopropyl 1-thio-β-D-galactoside was added to the culture to a final concentration of 0.4 mM when the cells reached an A_{600} of 0.6–0.8. The cells were harvested by centrifuging at 5000 × *g* for 20 min at 4 °C after 4 h of additional incubation at 37 °C. The pelleted cells were resuspended in the binding buffer (50 mM Tris-HCl, 0.5 M NaCl, 1% Triton X-100, pH 8.0) and sonicated briefly before centrifugation at 10,000 × *g* for 10 min at 4 °C. The supernatant was loaded on a nickel-charged His-Bind column according to the instructions provided by the manufacturer (Novagen) and purified by gel filtration on a Superdex 200 column (GE Healthcare).

Production of Nucleotide Sugars—UDP-4-keto-6-deoxyglucose (UDP-4K6DG) and UDP-Rha were enzymatically synthesized in our laboratory as neither is commercially available. UDP-4K6DG was synthesized using 20 μg of *in vitro* expressed RHM-N369 (31), and then the enzyme products were separated and purified by HPLC. UDP-Rha was synthesized by adding 20 μg of *in vitro* expressed UER1 to the reaction mixture (final volume, 0.5 ml) containing 6 mM

NADPH and 3 mM UDP-4K6DG. For production of UDP-Glc, 20 μg of purified UGP1 or UGP2 was added separately to reaction mixtures containing 3 mM UTP, 3 mM glucose 1-phosphate, and 3 mM $MgCl_2$. For UDP-GlcA production, 20 μg of purified UGD1 was added to the reaction mixture containing 6 mM NAD^+ and 3 mM UDP-Glc. For UDP-GalA production, 20 μg of purified GAE3 was added to the reaction mixture containing 3 mM UDP-GlcA. All reactions were incubated at 30 °C for 2 h in Na_3PO_4 buffer (pH ~7.0) and were stopped by adding ⅓ volume of $CHCl_3$.

HPLC Separation and GC/MS Identification—The water-soluble fractions obtained above were filtered with 0.22-μm filters (Millipore) and analyzed on an HPLC1200 series instrument (Agilent Technologies) at 40 °C using a ZORBAX Eclipse XDB-C_{18} column (0.46 × 15 cm; Agilent Technologies), monitored using a UV detector at 254 nm (32), and further identified by GC/MS as specified in the Analysis of Cell Wall Monosaccharide Composition section.

Ovule Culture and Chemical Treatment—UDP-Glc, UDP-GlcA, Rha, GlcA, and GalA were purchased from Sigma-Aldrich; UDP-GalA and UDP-Xyl were purchased from CarboSource Services. Cotton ovules (1 dpa) were collected, sterilized, and cultured in medium containing either 5 μM nucleotide sugars, free sugars, or C24:0 (Sigma-Aldrich) or 0.1 μM gaseous ethylene (99.9%; Qianxi Chemicals) in the head space at 30 °C in darkness. C24:0 was first dissolved in methyl *tert*-butyl ether (>99.0%) to 10 mM before being added to the culture to the final concentration as reported previously (12). All nucleotide or free sugars were first dissolved in double distilled H_2O to 5 mM and sterilized by passing through a 0.22-μm MILLEX filter (Millipore) before being diluted to specific concentrations in the culture medium. Where applicable, 1 μM ethylene perception inhibitor L-(2-aminoethoxyvinyl)glycine hydrochloride (AVG; >95.0%; Sigma) was also added to the ovule culture medium. The lengths (in mm) of the acidic water-straightened halo of fiber cells around each ovule (7) were measured manually under a dissecting microscope.

Uptake and Quantification of ^{14}C-Labeled Chemicals in Cotton Samples—^{14}C-Labeled UDP-GlcA, UDP-Xyl, and UDP-Glc were purchased from PerkinElmer Life Sciences. We enzymatically synthesized ^{14}C-labeled UDP-Rha using ^{14}C-labeled UDP-Glc in essentially the same way as reported under "Production of Nucleotide Sugars" because it is not commercially available. Cotton ovules were cultured in the same medium containing 1.66 nmol each of ^{14}C-labeled UDP-Rha (0.5 μCi), UDP-GlcA (0.3 μCi), or UDP-Xyl (0.24 μCi) separately for 6 days. Ovules were harvested and washed in double distilled H_2O three or four times until negligible amounts of the added radioactivity could be found in the wash. Total cell walls were isolated from cultured ovules, hydrolyzed thoroughly, and neutralized by exhaustive dialysis against double distilled H_2O before the radioactivity measurement. Pectins and hemicelluloses were extracted from cultured wild-type or *fl* ovules to determine the efficiency of chemical incorporation as described above.

Genetic Transformation of Arabidopsis, Molecular Characterization, and Root Hair Length Measurements—The cotton *UER1* (Gh *UER1c*) and *GAE3* (Gh *GAE3c*) cDNAs or the respective *Arabidopsis* genomic sequences (At *UER1g* and At *GAE6g*) were cloned under the control of the 1824-bp At *UER1* or 2002-bp At *GAE6* upstream promoter sequences and transformed into the homozygous *uer1-1* or *gae6-1* knock-out mutant lines. Genomic DNA was isolated using the DNeasy Plant kit (Qiagen), and 10 μg was digested with HindIII or BamHI and blotted for hybridization using a digoxigenin-labeled neomycin phosphotransferase II (NPTII) probe with the primers specified in supplemental Table 1.

For observation and measurements of root hairs, we followed a previously described method (33) and photographed the samples at 320× magnification using a stereomicroscope (Leica MZ APO). Fully grown hairs in the same root range (0.80 mm from the hair maturation region) were evaluated; we measured the lengths of six consecutive hairs protruding from each side of the primary roots. For each treatment or genotype, 15 roots with a total of 90 root hairs were scored.

Statistical Analysis—Whenever applicable, all data were evaluated by one-way analysis of variance software combined with Tukey's test to obtain *p* values.

RESULTS

Identification of Proteins and Significantly Up-regulated Biochemical Reactions in Wild-type Cotton Ovules—Comparative proteomics was carried out using cellular proteins extracted from 10-dpa cotton bolls (wild-type cv. Xuzhou 142) and the *fl* mutant (Fig. 1*A*). This particular mutant was used in an early microarray analysis that found the key importance of ethylene during cotton fiber cell elongation (7). As a result, about 1570 independent protein spots were observed on 2-DE gels of pH 4–7 and 3–10 with 103 spots present in significantly higher amounts ($p < 0.05$) in wild-type samples (supplemental Fig. 1; parts of the gels with pH 4–6.8 and 6.7–9 are shown). These 103 spots were excised, enzymatically digested, and subjected to MALDI-TOF MS identification. We identified 93 wild-type up-regulated polypeptides (Table I and supplemental Spectra 1), whereas eight of the spots (indicated by empty arrowheads in supplemental Fig. 1) could not be identified after repeated efforts. The two remaining spots (indicated by circles) that were more abundant in gels containing wild-type samples upon silver staining were not found after Coomassie Blue R-350 staining and thus were not subjected to MALDI-TOF MS analysis. Eleven wild-type down-regulated proteins, labeled from 94 to 104 in supplemental Fig. 1, were also identified. As indicated by the experimental pI and molecular mass in Table I, every protein came from a different spot in the proteome, and all identified polypeptides showed the best match to the corresponding cotton cDNA. Putative full-length cDNAs were obtained for all but one spot (FJ415211, spot 22) to reconfirm the newly identified cotton proteins (Table I). All identified peptide sequences are listed in supplemental Table 2.

Of the 104 identified proteins, 81 had E values higher than the cutoff in the KEGG pathway database, so they were subjected to KOBAS analysis. Nine biochemical pathways were found to be significantly up-regulated (FDR-corrected $p < 0.001$) during the fiber elongation period. Nucleotide sugar metabolism, which leads to cell wall polysaccharide biosynthesis, was ranked number one (supplemental Table 3).

Seven up-regulated proteins related to nucleotide sugar metabolism were further characterized by nano-LC-FTICR-MS or in some cases MALDI-TOF/TOF MS. Spots 32 and 33 were encoded by the same UDP-4-keto-6-deoxy-D-glucose 3,5-epimerase 4-reductase 1 gene (*UER1*), spots 79 and 80 were encoded by UDP-D-glucose pyrophosphorylase 1 (*UGP1*), spot 78 was encoded by *UGP2*, and spots 81 and 83 were encoded by the same UDP-D-glucose dehydrogenase 1 gene (*UGD1*) (supplemental Fig. 2 and supplemental Spectra 2). All four of these proteins were preferentially accumulated in

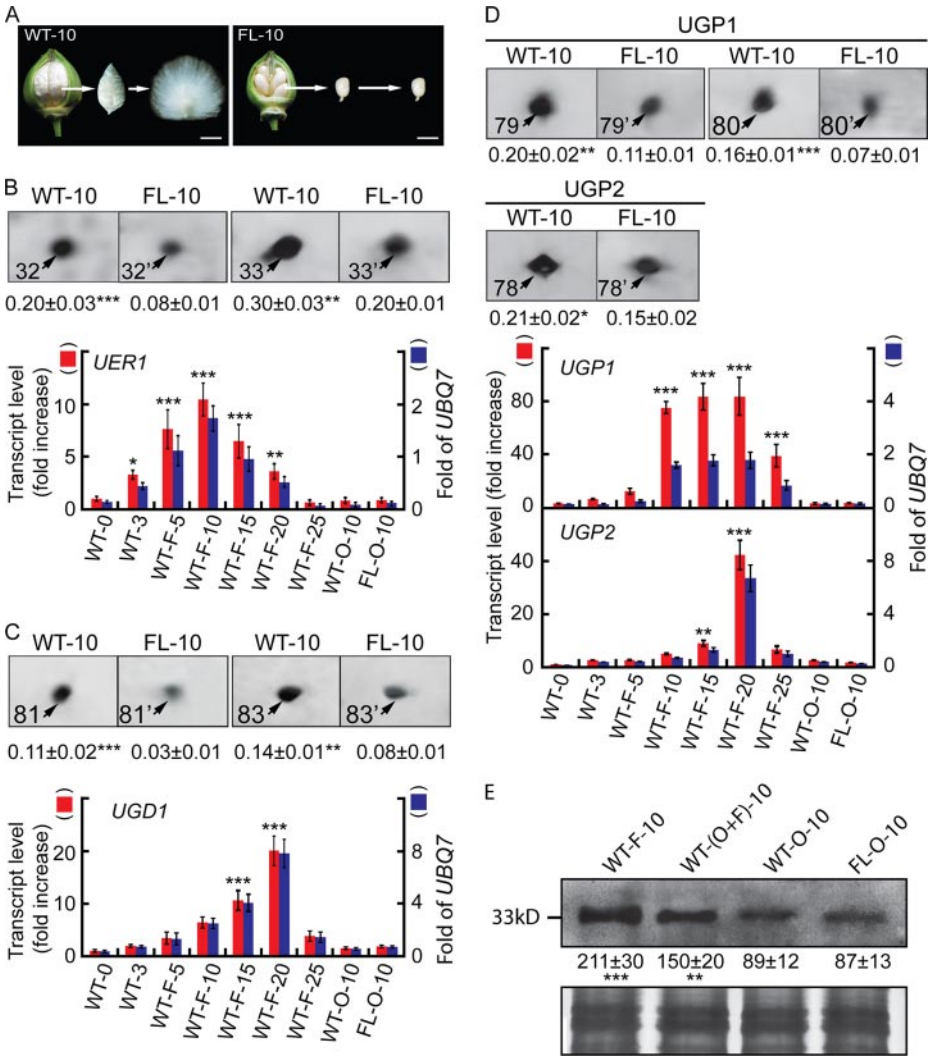

FIG. 1. **Analysis of proteins and transcripts preferentially accumulated during wild-type cotton ovule development.** *A*, phenotypes of 10-dpa wild-type (*left*) and *fl* mutant ovules (*right*). Fiber cells were combed upright to facilitate a visual comparison with the non-fibered mutant. *Scale bars*, 1.0 cm. *B*, more UER1 was present in wild-type preparations. *Upper panel*, protein spots 32 and 33 from 10-dpa wild-type (*WT-10*) and *fl* mutant (*FL-10*) ovule samples (see supplemental Fig. 1 for original 2-DEs). Means ± S.E. obtained from three independent 2-DEs with the total signal intensities of each gel set to 100 are reported *beneath* each protein spot. *Lower panel*, QRT-PCR of *UER1* transcripts. *Red bars* (*left* side scale) indicate increase relative to 0-dpa wild-type transcripts, which was arbitrarily set to 1. *Blue bars* (*right* side scale) indicate the amounts of *UER1* transcripts relative to cotton *UBQ7*. *WT-0* and *WT-3*, wild-type ovules harvested at 0 or 3 dpa with fiber initials attached; *WT-F-5*, *WT-F-10*, *WT-F-15*, *WT-F-20*, and *WT-F-25*, wild-type fibers harvested from 5 to 25 dpa; *WT-O-10* and *FL-O-10*, wild-type or *fl* mutant ovules harvested at 10 dpa. *, **, and ***, significant at $p < 0.05$, $p < 0.01$, and $p < 0.001$ levels, respectively. *Error bars* indicate standard deviations. *C*, more UGD1 was present in wild-type preparations. *D*, more UGPs were present in wild-type preparations. *C* and *D* are arranged in the same way as *B*. *E*, Western blotting using UER1-specific polyclonal antiserum. *Upper panel*, lanes were loaded with 20 μg of total protein extracted from 10-dpa cotton fibers (*F*), ovules with fibers attached (*O*+*F*), ovules with fibers removed (*O*), or mutant ovules (*FL-O*). Means ± S.E. of signal intensities were obtained from three independent experiments. *Lower panel*, part of the original Coomassie Blue R-350-stained SDS-PAGE.

wild-type proteomes (Fig. 1, *B–D*, *upper panels*) with significantly more transcripts found in fast elongating fibers as determined by QRT-PCR (Fig. 1, *B–D*, *lower panels*; see supplemental Table 1 for primer sequences). To confirm the strong expression of UER1 protein in wild-type 10-dpa cotton fibers, we performed Western blotting using antibodies produced from a synthesized polypeptide KESLIKYVFEPNKKT of UER1 (Fig. 1*E*). The cDNAs of full-length cotton *UER1*, *UGD1*, *UGP1*, and *UGP2* were amplified using primers reported in supplemental Table 1 before being cloned into pET28a upon sequence verification to produce pET28a-GhUER1, pET28a-GhUGD1, pET28a-GhUGP1, and pET28a-GhUGP2, respectively, with His_6 tags attached. Purified UER1, UGD1, UGP1, and UGP2 expressed *in vitro* possessed enzyme activities for the specific enzymatic reactions as expected, confirming their biochemical identities (supplemental Fig. 3, A–C).

TABLE I

MALDI-TOF MS identification of proteins preferentially accumulated in wild-type or in fl mutant cotton ovules

Spot no.[a]	Protein name	NCBI Accession no.	pI/exp.[b] molecular mass (kDa)	pI/theo.[c] molecular mass (kDa)	Score/cov.[d] (%)	Matched/ searched[e]	Relative protein content		Ratio WT/FL
							WT-10	FL-10	
1	Profilin	ABO43717	5.33/13.01	5.38/14.41	72/56	10/60	0.397 ± 0.034	0.205 ± 0.026	1.94
2[f]	Major latex-like protein	FJ415202	5.44/14.83	5.46/17.16	86/60	10/86	0.236 ± 0.028	0.121 ± 0.014	1.95
3	Annexin 1	AAR13288	6.31/15.81	6.19/36.15	172/55	20/64	0.103 ± 0.017	0.017 ± 0.009	6.06
6	Annexin	AAB67993	6.08/16.10	6.41/36.03	99/35	13/68	0.037 ± 0.005	0	[g]
18[f]	Annexin	FJ415173	6.52/28.49	6.74/35.98	123/38	14/60	0.065 ± 0.021	0.022 ± 0.008	2.95
5	Fiber annexin	AAC33305	6.11/16.04	6.34/36.21	99/37	15/81	0.075 ± 0.015	0.038 ± 0.011	1.97
4[f]	Copper,zinc-superoxide dismutase	FJ415203	5.83/15.98	5.47/15.36	106/92	10/59	0.162 ± 0.021	0.084 ± 0.025	1.93
7[f]	Copper,zinc-superoxide dismutase	FJ415203	5.83/16.35	5.47/15.36	88/92	10/93			
8[f]	Peroxiredoxin	FJ415174	5.35/17.41	5.58/17.30	140/74	10/44	0.127 ± 0.028	0.048 ± 0.008	2.65
9[f]	Dimethylmenaquinone methyltransferase	FJ415179	5.41/18.54	5.60/18.05	104/50	7/42	0.145 ± 0.023	0.080 ± 0.008	1.81
10	Benzoquinone reductase	ABN12321	6.09/21.65	6.09/21.65	69/39	5/49	0.295 ± 0.013	0.053 ± 0.007	5.57
13	Benzoquinone reductase	ABN12321	6.27/27.60	6.09/21.65	80/39	5/56			
14	Benzoquinone reductase	ABN12320	6.47/27.83	6.20/21.79	82/31	5/29	0.348 ± 0.039	0.034 ± 0.012	10.24
88[f]	Benzoquinone reductase	FJ415183	7.68/24.72	6.97/21.74	94/48	12/53	0.131 ± 0.019	0	[g]
11	Ascorbate peroxidase	ABR18607	5.13/27.49	5.93/27.74	84/52	9/50			
12	Ascorbate peroxidase	ABR18607	5.43/27.51	5.93/27.74	79/44	7/100			
15	Ascorbate peroxidase	ABR18607	5.68/27.84	5.93/27.74	90/46	6/77			
16	Ascorbate peroxidase	ABR18607	5.29/27.87	5.93/27.74	78/47	9/59	0.239 ± 0.025	0.040 ± 0.017	5.98
19	Ascorbate peroxidase	ABR18607	5.32/28.70	5.93/27.74	101/49	9/51			
20	Ascorbate peroxidase	ABR18607	5.64/28.75	5.93/27.74	151/64	15/41			
21	Ascorbate peroxidase	ABR18607	5.15/29.28	5.62/27.58	112/60	13/67			
17[f]	Ascorbate peroxidase	FJ415185	4.96/27.89	5.62/27.58	66/38	5/60	0.207 ± 0.032	0.043 ± 0.015	4.81
38[f]	Stromal ascorbate peroxidase	FJ415186	6.24/36.78	8.89/41.05	85/35	13/75	0.102 ± 0.014	0.047 ± 0.015	2.17
40[f]	Stromal ascorbate peroxidase	FJ415186	6.10/37.04	8.89/41.05	73/28	9/100			
22[f]	α-1,4-glucan phosphorylase	FJ415211	4.94/30.21	5.32/10.67	108/23	19/94	0.132 ± 0.010	0	[g]
23[f]	*S*-Formylglutathione hydrolase	FJ415188	6.59/30.65	6.82/32.18	77/47	10/89	0.120 ± 0.036	0.050 ± 0.002	2.40
24[f]	Triose-phosphate isomerase	FJ415177	6.53/31.54	6.00/27.47	142/82	15/110	0.253 ± 0.035	0.170 ± 0.019	1.49
25[f]	20 S proteasome subunit α-1	FJ415181	6.44/31.80	5.91/27.39	112/47	11/49	0.105 ± 0.009	0.035 ± 0.01	3.00
26[f]	Heat shock protein 70	FJ415196	6.27/32.83	5.07/71.57	74/19	9/77	0.146 ± 0.010	0.036 ± 0.025	4.06
68[f]	Heat shock protein 70	FJ415196	4.75/52.95	5.10/71.37	84/26	15/99			
63[f]	Heat shock protein 70	FJ415199	4.59/49.92	5.10/71.35	88/27	9/95	0.113 ± 0.007	0.043 ± 0.041	2.63
67[f]	Heat shock protein 70	FJ415194	4.69/52.90	5.14/71.28	89/21	9/37	0.468 ± 0.027	0.134 ± 0.030	3.49
90[f]	Heat shock protein 70	FJ415194	7.52/33.12	5.14/71.28	84/20	9/65			
73[f]	Heat shock protein 70	FJ415195	4.75/54.07	5.07/71.57	90/13	8/47	0.059 ± 0.007	0.010 ± 0.011	5.90
27[f]	Catalase	FJ415187	6.30/33.59	6.68/57.25	73/30	16/84	0.197 ± 0.032	0.091 ± 0.015	2.16
28[f]	Serine hydroxymethyltransferase	FJ415180	5.54/34.18	7.57/52.38	95/26	9/59	0.091 ± 0.008	0.014 ± 0.001	6.50
31[f]	Serine hydroxymethyltransferase	FJ415180	5.83/34.82	7.57/52.38	75/36	12/76			
29[f]	Lactoylglutathione lyase	FJ415204	5.71/34.38	5.69/32.61	69/34	11/69	0.202 ± 0.016	0	[g]
30[f]	α-Soluble NSF[h] attachment protein	FJ415171	5.08/34.75	5.11/33.05	120/39	9/23	0.110 ± 0.033	0.034 ± 0.012	3.24
32[f]	UER1	FJ415167	5.94/34.94	5.73/33.95	180/62	18/79	0.253 ± 0.030	0.253 ± 0.030	1.78
33[f]	UER1	FJ415167	6.22/34.97	5.73/33.95	215/64	15/31			
34[f]	Fructokinase	FJ415169	5.05/36.08	5.28/35.20	206/58	16/41	0.080 ± 0.002	0.045 ± 0.009	1.78
35	Enolase	ABW21688	5.21/36.28	5.49/47.98	85/29	7/78	0.049 ± 0.003	0	[g]
36	Actin	AAP73454	5.43/36.64	5.23/41.90	90/46	12/63	0.178 ± 0.027	0.027 ± 0.028	6.59
52	Actin	AAP73452	5.62/42.35	5.44/41.94	69/29	7/86	0.264 ± 0.017	0.018 ± 0.020	14.67
53	Actin	AAP73457	5.56/43.29	5.31/41.91	149/60	28/142	0.244 ± 0.03	0.039 ± 0.036	6.26
71	Actin	AAP73460	5.45/53.58	5.37/41.94	163/57	22/91	0.189 ± 0.023	0.120 ± 0.032	1.58
37[f]	Granule-bound starch synthase	FJ415189	4.97/36.64	8.79/63.84	80/20	8/55	0.087 ± 0.012	0	[g]
39[f]	Granule-bound starch synthase	FJ415205	4.91/36.78	8.59/67.73	135/35	13/89	0.090 ± 0.016	0.019 ± 0.011	4.76
41[f]	Glutamine synthase	FJ415178	5.64/37.12	5.77/39.36	140/43	10/50	0.078 ± 0.006	0	[g]
42[f]	Malate dehydrogenase	FJ415192	6.14/38.50	6.10/36.45	93/27	10/77	0.337 ± 0.004	0.222 ± 0.028	1.52

TABLE I—*continued*

Spot no.[a]	Protein name	NCBI Accession no.	pI/exp.[b] molecular mass (kDa)	pI/theo.[c] molecular mass (kDa)	Score/cov.[d] (%)	Matched/ searched[e]	Relative protein content		Ratio WT/FL
							WT-10	FL-10	
56[f]	Malate dehydrogenase	FJ415192	6.67/46.15	6.10/35.87	88/43	8/100			
43	Phenylcoumaran benzylic ether reductase-like protein	ABN12322	5.58/38.89	5.76/33.89	92/35	11/48	0.227 ± 0.021	0.102 ± 0.022	2.23
51	Phenylcoumaran benzylic ether reductase-like protein	ABN12322	5.87/41.46	5.76/33.89	129/58	18/97			
45	β-Tubulin 19	ABY86665	5.75/39.76	4.76/50.65	173/58	26/70	0.073 ± 0.034	0	[g]
46	α-Tubulin 4	AAN33000	5.57/39.90	5.36/34.41	207/64	19/40	0.145 ± 0.007	0.059 ± 0.018	2.46
49	α-Tubulin 4	AAN33000	5.43/40.90	5.36/34.41	107/44	12/65			
48	α-Tubulin	ABO47738	5.72/40.45	4.97/50.29	159/43	19/38	0.155 ± 0.029	0	[g]
50[f]	Glyceraldehyde-3-phosphate dehydrogenase C subunit	FJ415206	6.61/41.24	7.70/36.65	73/33	7/87	0.234 ± 0.030	0.115 ± 0.052	2.04
54[f]	2-Nitropropane dioxygenase	FJ415176	5.43/43.73	5.32/36.17	211/68	18/62	0.330 ± 0.009	0.134 ± 0.033	2.46
55[f]	Quinone oxidoreductase	FJ415175	5.21/45.90	5.28/34.39	149/67	16/106	0.088 ± 0.014	0	[g]
57	Gibberellin 20-oxidase 1	ABA01482	5.23/48.01	5.35/41.72	215/64	24/84	0.030 ± 0.007	0	[g]
58	Flavanone 3-hydroxylase	ABM64799	5.33/48.10	5.43/41.75	171/66	26/130	0.485 ± 0.007	0.226 ± 0.023	2.14
59[f]	Mannitol dehydrogenase	FJ415191	5.93/49.11	5.85/39.57	100/61	16/90	0.252 ± 0.032	0.144 ± 0.026	1.75
60[f]	Adenosine kinase	FJ415170	5.46/49.66	5.47/37.81	200/59	15/38	0.059 ± 0.018	0.145 ± 0.028	1.40
61[f]	Adenosine kinase	FJ415170	5.31/49.66	5.47/37.81	128/55	18/64			[g]
62[f]	Phosphoglycerate dehydrogenase	FJ415190	5.20/49.84	7.14/64.06	81/23	7/54	0.111 ± 0.009	0	[g]
65[f]	Phosphoglycerate dehydrogenase	FJ415190	5.13/50.35	7.14/64.06	77/27	8/100			
64[f]	Pyruvate dehydrogenase α subunit	FJ415197	6.74/50.17	7.16/43.69	79/30	9/100	0.222 ± 0.013	0.157 ± 0.008	1.41
66	Anthocyanidin reductase	ABM64802	5.53/51.74	5.54/36.54	138/49	16/86	0.358 ± 0.003	0	[g]
69[f]	Luminal binding protein	FJ415200	4.57/53.09	5.13/73.57	81/31	17/95	0.062 ± 0.016	0.015 ± 0.012	4.13
70[f]	Luminal binding protein	FJ415200	4.50/53.55	5.13/73.57	76/23	9/100			
72[f]	Luminal binding protein	FJ415200	4.55/53.94	5.13/73.57	104/25	10/67			
74[f]	Phosphoglycerate kinase	FJ415172	6.14/56.40	5.97/42.29	140/44	14/59	0.063 ± 0.008	0.035 ± 0.003	1.80
75	Chloroplast biotin carboxylase	ABP98813	6.30/57.92	7.57/59.17	94/34	19/85	0.083 ± 0.011	0.049 ± 0.010	1.69
77	Chloroplast biotin carboxylase	ABP98813	6.31/59.64	7.57/59.17	139/61	26/101			
76[f]	Dihydrolipoamide dehydrogenase	FJ415193	6.62/59.37	6.93/54.13	70/25	8/100	0.118 ± 0.026	0	[g]
78[f]	UGP2	FJ415165	5.54/60.41	5.62/51.45	155/49	18/100	0.205 ± 0.015	0.145 ± 0.023	1.42
79[f]	UGP1	FJ415164	6.07/61.70	5.81/51.74	132/52	17/61	0.178 ± 0.016	0.092 ± 0.014	1.93
80[f]	UGP1	FJ415164	6.10/61.70	5.81/51.74	216/61	22/63			
81[f]	UGD1	FJ415166	6.11/62.84	5.84/53.64	183/59	23/109	0.124 ± 0.016	0.057 ± 0.013	2.18
83[f]	UGD1	FJ415166	6.30/64.12	5.84/53.64	188/53	18/49			
82[f]	*myo*-Inositol-1-phosphate synthase	FJ415168	5.69/63.53	5.46/56.54	207/54	24/106	0.090 ± 0.006	0.046 ± 0.010	1.96
84	Acyltransferase-like protein	AAL67994	5.67/64.47	5.67/48.29	107/40	22/108	0.100 ± 0.013	0.019 ± 0.008	5.26
85	Acyltransferase-like protein	AAL67994	5.56/64.82	5.67/48.29	72/38	15/110			
86[f]	Pyruvate decarboxylase	FJ415201	6.57/69.52	6.13/60.77	99/30	11/100	0.128 ± 0.033	0.025 ± 0.014	5.00
87[f]	Glycine-rich RNA-binding protein	FJ415184	7.82/15.01	7.82/17.08	111/62	13/72	0.116 ± 0.030	0	[g]
89	Manganese-superoxide dismutase	AAC78469	7.49/25.40	8.54/22.14	158/75	16/100	0.089 ± 0.015	0.041 ± 0.008	2.17
91[f]	Glyceraldehyde-3-phosphate dehydrogenase	FJ415182	7.74/43.72	7.06/37.04	92/58	15/100	0.167 ± 0.023	0.048 ± 0.015	3.48
92[f]	Isocitrate dehydrogenase	FJ415198	7.32/53.15	6.29/46.41	188/63	28/100	0.381 ± 0.030	0.256 ± 0.029	1.49
93[f]	Isocitrate dehydrogenase	FJ415198	7.07/53.29	6.29/46.41	140/57	23/100			
94[f]	Eukaryotic translation initiation factor 5A	GU295062	5.55/18.88	5.61/17.63	96/52	9/61	0.156 ± 0.026	0.293 ± 0.024	0.53
95[f]	Chalcone isomerase	GU295063	4.84/29.85	4.85/23.42	95/67	10/66	0.104 ± 0.021	0.177 ± 0.017	0.59
96[f]	Triose-phosphate isomerase	GU295064	5.52/30.18	6.66/33.50	101/53	16/138	0.051 ± 0.009	0.122 ± 0.016	0.42
97[f]	Thiazole biosynthetic enzyme	GU295068	5.03/36.81	5.64/38.24	170/63	17/49	0.048 ± 0.008	0.155 ± 0.024	0.31
98[f]	Transaldolase	GU295065	4.91/45.56	5.78/43.06	129/33	10/18	0.036 ± 0.005	0.089 ± 0.012	0.40
100[f]	Transaldolase	GU295065	5.09/46.62	5.78/43.06	123/29	12/32			

TABLE I—*continued*

Spot no.[a]	Protein name	NCBI Accession no.	pI/exp.[b] molecular mass (kDa)	pI/theo.[c] molecular mass (kDa)	Score/cov.[d] (%)	Matched/ searched[e]	Relative protein content		Ratio WT/FL
							WT-10	FL-10	
99[f]	U2 small nuclear ribonucleoprotein A	GU295066	5.06/45.90	4.97/32.19	204/68	18/50	0.062 ± 0.003	0.237 ± 0.033	0.26
101	Chalcone synthase	ABS52573	6.11/54.17	6.12/42.98	87/35	11/45	0.039 ± 0.010	0.104 ± 0.026	0.38
102	Protein-disulfide isomerase	ABO41843	5.01/65.30	5.07/55.89	203/59	24/77	0.051 ± 0.010	0.102 ± 0.003	0.50
103[f]	RNA helicase-like protein	GU295067	5.91/69.24	5.65/56.15	201/43	17/32	0.062 ± 0.012	0.121 ± 0.020	0.51
104	Betaine-aldehyde dehydrogenase	AAR23816	5.44/69.43	5.60/55.37	100/42	19/103	0.055 ± 0.011	0.114 ± 0.012	0.48

[a] Protein spots are arranged from lowest to highest molecular mass with spots encoded by the same cotton cDNA quantified as one protein and spots presumably encoded by the same gene family located next to each other. Spots 1–93 were preferentially accumulated in the wild type, and spots 94–104 were preferentially accumulated in the mutant.
[b] Experimental.
[c] Theoretical.
[d] Coverage.
[e] Number of matched/searched polypeptides.
[f] Sixty-eight polypeptides encoded by 50 putative full length and one partial (spot 22, FJ415211) cotton cDNAs obtained for the first time in the current work.
[g] Protein spots only observed in WT-10.
[h] *N*-Ethylmaleimide-sensitive factor.

Exogenous Ethylene and C24:0 Result in Accumulation of UER1, UGP1, and UGD1 at Protein and Transcript Levels—Because ethylene is known to promote fiber elongation (7) and its production in cotton is regulated by C24:0 (12), we performed another set of comparative proteomics using 1-dpa cotton ovules treated with 0.1 μM ethylene or 5 μM C24:0 for 24 h (supplemental Fig. 4). The levels of UER1, UGD1, and UGP1 increased significantly in wild-type samples after both treatments, whereas no such change was observed in mutant ovules (Fig. 2, *A–C*). QRT-PCR analysis indicated that *UER1*, *UGD1*, and *UGP1* transcripts increased significantly as soon as 3–6 h after inclusion of either chemical in wild-type ovule culture (Fig. 2, *D–F*). UGP2 did not respond to either treatment at the protein or transcript level (Fig. 2, *C* and *F*, *lower panels*). By contrast, 48–72 h were required for either chemical to promote significant fiber cell growth (Fig. 2*G*). Addition of either UDP-Rha or UDP-GalA to ovule culture medium reversed the growth-inhibitory effect brought about by the ethylene perception inhibitor AVG (Fig. 2*H*), indicating that ethylene promotes fiber growth mainly through activation of pectin biosynthesis.

Further QRT-PCR analysis revealed that all four bifunctional rhamnose synthase (RHM) isoforms, which may function alone to synthesize UDP-Rha, from the cotton genome were expressed at relatively fixed levels in the plant with no fiber preference (supplemental Fig. 5A) and were not activated upon ethylene treatment (supplemental Fig. 5B). These data suggest that additional UER activities, which depend on the UDP-D-Glc 4,6-dehydratase function of RHMs, may be required to sustain the specialized cotton fiber cell elongation.

Fiber Cell Walls Contain Significantly Higher Amounts of Pectic Components than Those of Ovule Cells—Consistent with the highly preferentially accumulated proteins that synthesize two types of pectin precursors, elongating fiber cells contained higher amounts of pectin and less hemicellulose than both wild-type and *fl* mutant ovules harvested at the same growth stage (Fig. 3*A*). GC/MS analysis of the non-cellulose neutral sugars indicated that more rhamnose and arabinose were found per gram of fiber cell wall preparations, whereas more xylose and glucose were produced in ovule samples of both genotypes (Fig. 3*B*). When purified pectin and hemicellulose were analyzed further using the same GC/MS program, most of the rhamnose and arabinose were present in the pectin fraction, whereas xylose and glucose were mainly in the hemicellulose fraction (Fig. 3*C*). Fiber cell walls contained significantly higher levels of GalA than ovule samples, whereas very low and non-variable amounts of GlcA were present in all three samples (Fig. 3*D*). Although the dimethyl sulfoxide added at the time of cell wall extraction may affect the solubility of various cell wall carbohydrates, the degree of influence should be the same to both wild-type and mutant cell walls.

Pectin Precursors Promote Cotton Fiber Growth—Because UDP-Rha, UDP-GlcA, and UDP-GalA are the primary nucle-

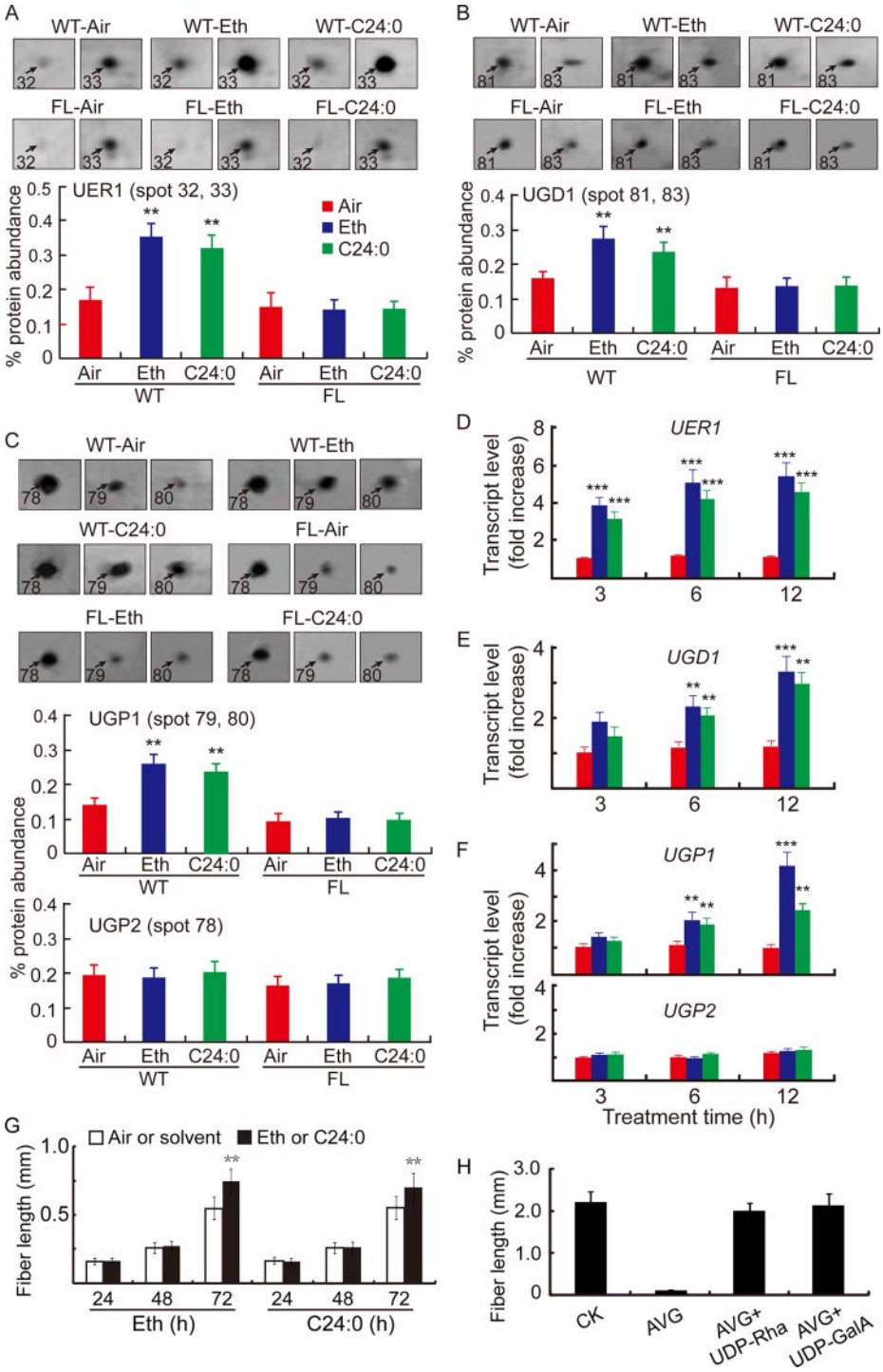

FIG. 2. **Ethylene and C24:0 stimulate UER1, UGD1, and UGP1 accumulation both at mRNA and protein levels in wild-type cotton ovules.** *A*, analysis of UER1 content after control (*Air*), ethylene (*Eth*), or lignoceric acid (*C24:0*) treatment. Protein samples prepared from 1-dpa wild-type ovule samples cultured in the presence of 0.1 μM ethylene or 5 μM C24:0 or in the absence of these chemicals (*Air*) for 24 h were loaded onto a series of 2-DE gels (supplemental Fig. 4). Shown are representative protein spots 32 and 33 (following the same numbering system as in supplemental Fig. 1) upon the various treatments (*upper panel*) and quantification of the signal intensities reported as the sum of both spots (mean ± S.E.) obtained from three independent 2-DEs (*lower panel*). Similar treatments were performed and reported using mutant (*FL*) ovules. *B*, analysis of UGD1 after control, ethylene, or C24:0 treatment. *C*, analysis of UGP1 and UGP2 after control, ethylene, or C24:0 treatment. *B* and *C* are arranged in the same way as *A*. *D*, QRT-PCR analysis of *UER1* transcripts from WT ovules after 3, 6, and 12 h of control, ethylene, or C24:0 treatment. RNA samples from WT ovules were cultured for the same period of time without addition of ethylene or C24:0 were used as controls. *E*, QRT-PCR analysis of *UGD1* transcripts upon control, ethylene, or C24:0 treatment. *F*, QRT-PCR analysis of *UGP1* and *UGP2* transcripts upon control, ethylene, or C24:0 treatment. *Bars* in *D*, *E*, and *F* are color-coded as in *A*. *G*, fiber lengths from *in vitro* cultured wild-type cotton ovules after ethylene or C24:0 treatment for a specified period of time (h). *H*, the inhibitory effect of AVG was significantly reversed by adding either 5 μM UDP-Rha or 5 μM UDP-GalA to the growth medium. All experiments were repeated three times using independent cotton materials and reported as mean ± S.E. *Error bars* indicate standard deviations. See the legend to Fig. 1 for details regarding QRT-PCR and statistical performance.

otide sugar substrates used for pectic polymer biosynthesis (see the scheme provided in supplemental Fig. 6 that was reproduced with permission from Ref. 34), these substrates were exogenously applied to the ovule culture medium. Each substrate promoted significant fiber cell elongation (Fig. 4*A*). By contrast, UDP-Glc promoted fiber cell elongation to a significantly lower degree when it was applied to the ovule culture medium (Fig. 4*A*), indicating that the conversion from UDP-Glc to UDP-Rha or UDP-GalA is important for fiber growth. The same amount of UDP-Xyl (a precursor for hemicellulose) or free Rha, GlcA, and GalA was ineffective in the same growth assay (Fig. 4*A*). UDP-GalA is synthesized from UDP-GlcA by the enzyme UDP-D-glucuronic acid 4-epimerase (GAE), which is a Golgi-localized protein (35) and is not part of our proteome. To determine a potential role for GAE in fiber cell growth, we cloned all five *GAE* homologs available in

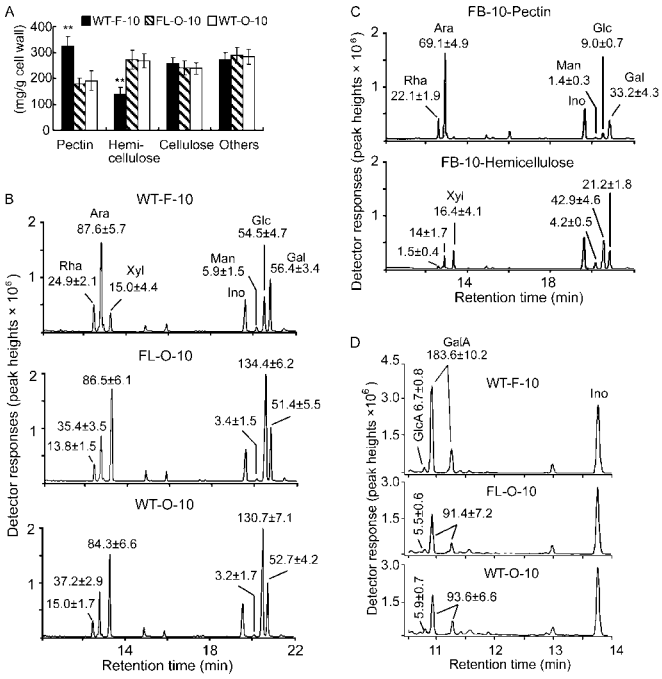

FIG. 3. **Quantitative analysis of cell wall polysaccharide compositions, neutral sugars, and uronic acid contents.** *A*, determination of the relative amounts of pectin, hemicellulose, cellulose, and other unidentified components (*Others*) from cell wall materials of 10-dpa cotton fibers (*F-10*) or ovules (*O-10*) of wild type (*WT*) and the *fl* mutant (*FL*). **, significant at $p < 0.01$. *Error bars* indicate standard deviations. *B*, GC/MS separation and identification of neutral sugars. Thoroughly hydrolyzed and alditol acetate-derivatized non-cellulose cell wall polymers isolated from 10-dpa fiber cells (*WT-F-10*; *upper panel*) and ovules harvested at 10 dpa (*FL-O-10* and *WT-O-10*; *middle* and *lower panels*, respectively) were analyzed by GC/MS. Inositol (*Ino*) was added at the time of extraction as an internal control. The spectra represent results obtained from three independent experiments using different cotton materials. *Ara*, arabinose; *Man*, mannose; *Glc*, glucose; *Gal*, galactose. *C*, GC/MS analysis of neutral sugars from purified pectin (*FB-10-Pectin*; *upper panel*) and hemicelluloses (*FB-10-Hemicellulose*; *lower panel*) using 10-dpa fiber cell wall isolations. *D*, GC/MS analysis of uronic acid composition in non-cellulose cell wall fractions. The entire experiment was repeated three times using independent cotton materials, and the data are reported at the *top* of each corresponding peak as mean ± S.E. (mg/g of cell wall).

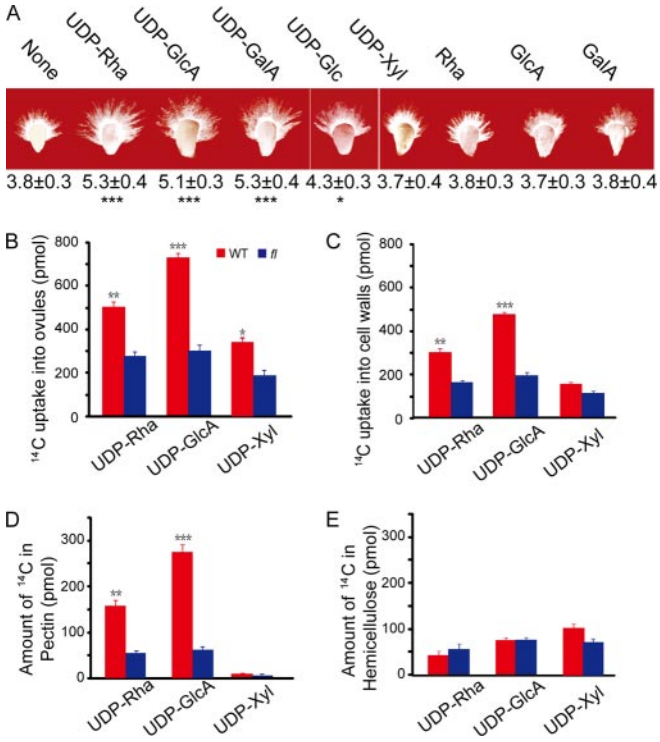

FIG. 4. **Growth stimulation and sufficient incorporation of applied nucleotide sugars into pectins.** *A*, phenotypes of wild-type ovules collected at 1 dpa and cultured in the presence of 5 μM UDP-Rha, UDP-GlcA, UDP-GalA, UDP-Glc, or UDP-Xyl or in the same concentration of free Rha, GlcA, or GalA for 6 days. The measurements (mean ± S.E. in mm) are shown *below* each representative ovule. * and ***, significant at $p < 0.05$ and $p < 0.001$ levels, respectively. *None*, no extra chemical added. *B*, wild-type cotton ovules with growing fibers took up significantly more ^{14}C-labeled nucleotide sugars than *fl* ovules. Chemical uptake was calculated by subtracting the radioactivity remaining in the medium and in the wash from the amount of radiolabels applied initially in each culture. *Error bars* indicate standard deviations. *C*, most of the radiolabel from the exogenous nucleotide sugar feeding experiments was recovered in cotton fiber cell walls. *D*, the majority of the exogenous UDP-Rha and UDP-GlcA was incorporated into pectic polymers. *E*, UDP-Xyl was incorporated mainly into hemicelluloses.

a cotton cDNA microarray (Gene Expression Omnibus (GEO) accession number GPL5476) containing 31,401 UniESTs in combination with data available from NCBI (www.ncbi.nlm.nih.gov/sites/entrez?term=gossypium&cmd=Search&db=nucest). QRT-PCR experiments indicated that the most actively transcribed *GAE3* was highly preferentially expressed in fast elongating fiber cells (supplemental Fig. 7). We also confirmed the functionality of GAE3 using an *in vitro* enzyme activity assay (supplemental Fig. 3D).

Cotton Fibers Take Up Significantly More ^{14}C-Labeled Pectin Precursors than Do Ovule Cells—When cultured in the presence of various ^{14}C-labeled chemicals for 6 days, 30–43% of the total radiolabel from UDP-Rha and UDP-GlcA was recovered in wild-type cotton ovules. By contrast, only about 20% of the initial label from UDP-Xyl was recovered in wild-type cotton ovules (Fig. 4*B*). Mutant ovules took up significantly less of the initial label from each chemical in the same assay (Fig. 4*B*), indicating that elongating fiber cells, not ovule cells, actively and selectively absorb nucleotide sugars that serve as immediate pectin precursors. Greater than 60% of the radiolabels from exogenous nucleotide sugar feeding experiments was recovered in cell wall extracts (Fig. 4*C*) with the majority of the radiolabels from UDP-Rha and UDP-GlcA found in pectin fractions and that of UDP-Xyl found in hemicellulose fractions (Fig. 4, *D* and *E*).

Genetic Complementation of uer1-1 and gae6-1 Arabidopsis Knock-out Mutants by Respective Cotton cDNA—Two *Arabidopsis* knock-out mutants, *uer1-1* (At1g63000, encoding the *Arabidopsis* UDP-4-keto-6-deoxy-D-glucose 3,5-epim-

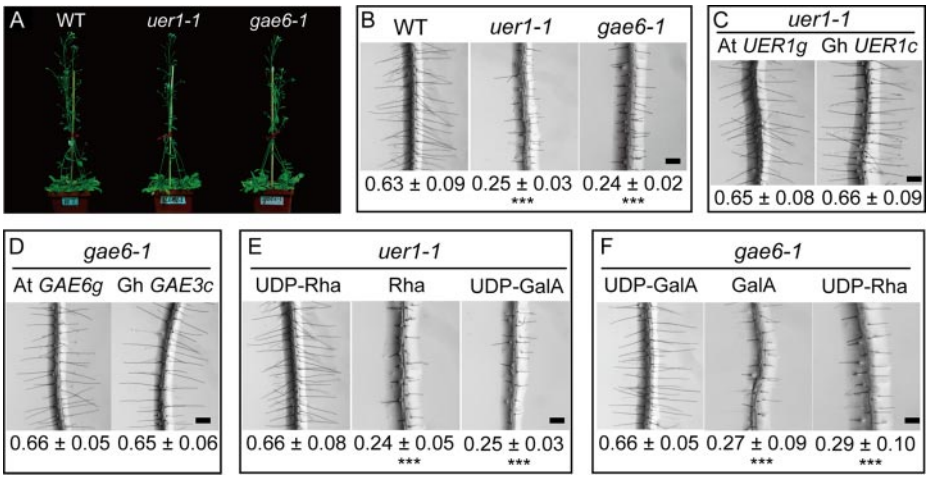

FIG. 5. ***Arabidopsis uer1-1* and *gae6-1* mutants were genetically or chemically complemented by expressing a specific cotton cDNA or by supplementing the respective nucleotide sugars in growth medium.** *A*, phenotypes of wild-type Col, *uer1-1*, and *gae6-1* plants at the time of flowering. *B*, close-up views taken from the fully elongated root hair zone of 10-day-old *Arabidopsis* seedlings (mean ± S.E. in mm). *C*, wild-type root hairs were produced on T2 transgenic *Arabidopsis* seedlings expressing either At *UER1g* (*left*) or Gh *UER1c* (*right*). *D*, wild-type root hairs were produced on T2 transgenic *Arabidopsis* seedlings expressing either At *GAE6g* (*left*) or Gh *GAE3c* (*right*). *E*, 5 μM exogenous UDP-Rha (*left*), but not free Rha (*middle*) or UDP-GalA (*right*), chemically complemented the root hair phenotype of *uer1-1*. *F*, 5 μM exogenous UDP-GalA (*left*), but not free GalA (*middle*) or UDP-Rha (*right*), chemically complemented the root hair phenotype of *gae6-1*. *Scale bars* in *B–F*, 200 μm. ***, significant at $p < 0.001$ compared with the wild type.

erase 4-reductase 1 gene) and *gae6-1* (At3g23820, encoding the *Arabidopsis* UDP-D-glucuronic acid 4-epimerase 6 gene), orthologs of cotton *UER1* and *GAE3*, respectively, were obtained from Salk Institute Genomic Analysis Laboratory collections (*Arabidopsis* Biological Resource Center; http://signal.salk.edu). In each line, a single T-DNA insertion, as verified by genomic PCR and subsequent Southern blot, resulted in complete loss of target gene expression (supplemental Figs. 8 and 9). Apart from being slower than the wild type in the initial stages of development (until reproductive growth), the mutants did not show significant changes of whole-plant architecture (Fig. 5*A*). Similar observations were reported in a number of *gaut1 Arabidopsis* mutants that lack the enzyme to transfer D-galacturonic acid residues from UDP-GalA to the pectic polysaccharide homogalacturonan (36). However, when we examined root hair growth, which is a result of rapid linear outgrowth of epidermal cells similar to cotton fibers, both these mutants showed significantly shorter root hairs than the wild type as observed in close-up views under a dissecting microscope (Fig. 5*B*). When a functional genomic *Arabidopsis UER1* clone (Fig. 5*C*, *left*) or the cotton *UER1* cDNA (Fig. 5*C*, *right*) under the control of the same 1824-bp *Arabidopsis UER1* upstream sequence was transformed into the *uer1-1* genetic background, wild-type lengths of root hairs were observed (Fig. 5*C*). The root hair phenotypes observed in *gae6-1* were also genetically complemented by a functional genomic *Arabidopsis GAE6* clone (Fig. 5*D*, *left*) or cotton *GAE3* cDNA (Fig. 5*D*, *right*) controlled by the same 2002-bp *Arabidopsis GAE6* upstream sequence (Fig. 5*D*).

Complementation of Short Root Hair Phenotypes of uer1-1 and gae6-1 by Exogenous UDP-Rha or UDP-GalA—Wild type-like root hairs were produced from *uer1-1* plants when 5 μM exogenous UDP-Rha was included in solid ½ Murashige and Skoog medium (Fig. 5*E*, *left*). Likewise, 5 μM exogenous UDP-GalA rescued the root hair phenotypes of *gae6-1* (Fig. 5*F*, *left*). Addition of UDP-GalA to *uer1-1* plants or UDP-Rha to *gae6-1* plants did not compensate for the growth deficit (Fig. 5, *E* and *F*, *right*), suggesting that pectin precursors relevant to the respective biochemical steps are important for *Arabidopsis* root hair elongation. In either case, the same amount of free Rha or free GalA did not complement the hair growth deficits (Fig. 5, *E* and *F*, *middle*).

Specific Combinations of Nucleotide Sugars Rescue Short Root Hair Phenotypes of Two Additional Arabidopsis Mutants—Significantly shorter root hairs were found in two additional *Arabidopsis* mutant lines, *ein2-5*, a mutant in ethylene signaling (37), and *cut1*, a mutant in the very-long-chain fatty acid biosynthesis pathway (38) that is necessary for activating ethylene production during cotton fiber growth (12). Using total RNA prepared from the roots of *ein2-5* and *cut1* mutants, we found that the expression of both *UER1* and *GAE6* was significantly reduced in each mutant background (Fig. 6, *A* and *B*). A similar inhibitory pattern of *UER1* and *GAE6* expression is found in large scale microarray experiments using mutant RNA samples (https://www.genevestigator.com/ and https://www.weigelworld.org/resources/microarray/AtGenExpress/). Significant elongation of *ein2-5* and *cut1* root hairs was observed when 5 μM UDP-Rha or UDP-GalA was applied to solid ½ Murashige and Skoog medium (Fig. 6, *C* and *D*). In either

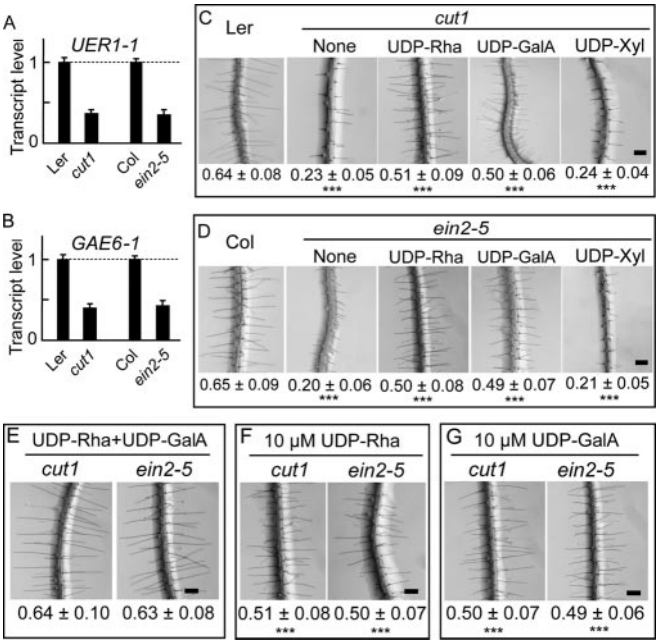

FIG. 6. **Wild-type root hair lengths were produced in *cut1* and *ein2-5 Arabidopsis* mutants by addition of exogenous nucleotide sugars required for different pectic polymer biosyntheses.** *A*, QRT-PCR analysis of *UER1* transcripts in *cut1* and *ein2-5 Arabidopsis* mutants. *B*, QRT-PCR analysis of *GAE6* transcripts in the mutants. *Error bars* indicate standard deviations. *C*, 5 μM UDP-Rha or UDP-GalA applied to the growth medium promoted significant *cut1* root hair elongation. Addition of the same amount of UDP-Xyl to the growth medium did not promote root hair elongation compared with the control that received no extra chemical (*None*). Mean ± S.E. of root hair length (in mm) is shown *below* each image. ***, significant at $p < 0.001$ compared with wild-type Ler root hairs. *D*, 5 μM UDP-Rha or UDP-GalA applied to the growth medium promoted significant *ein2-5* root hair elongation. ***, significant at $p < 0.001$ compared with wild-type Col root hairs. *E*, wild-type root hair lengths were produced from *cut1* and *ein2-5* plants when a combination of 5 μM UDP-Rha and 5 μM UDP-GalA (*UDP-Rha+UDP-GalA*) were added to the growth medium. *F*, addition of 10 μM UDP-Rha did not support further root hair growth in either mutant. *G*, addition of 10 μM UDP-GalA did not support further root hair growth in either mutant. *Scale bars* in *C–G*, 200 μm. ***, significant at $p < 0.001$ compared with wild-type root hairs.

case, addition of one nucleotide sugar did not result in wild-type root hair lengths on the mutant. The same amount of UDP-Xyl in the medium showed no effect on the growth of root hairs of either mutant (Fig. 6, *C* and *D*). A combination of 5 μM UDP-Rha and 5 μM UDP-GalA resulted in wild-type root hair lengths of both *ein2-5* and *cut1* plants (Fig. 6*E*). By contrast, addition of 10 μM UDP-Rha or UDP-GalA alone did not produce the same stimulatory effect (Fig. 6, *F* and *G*), suggesting that different types of nucleotide sugars synthesized via UGP/UER and UGD/GAE are necessary for *Arabidopsis* root hair growth.

DISCUSSION

A total of 104 polypeptides, with 93 preferentially accumulated in wild-type and 11 preferentially accumulated in mutant samples, were identified by comparing the 2-DE maps of these cotton materials. Analysis of the identified biochemical reactions, with reference to the *Arabidopsis* genome, revealed that nucleotide sugar metabolism was activated most significantly during cotton fiber cell elongation. Fiber-preferential accumulation of UGP was also reported previously (39). Up-regulated protein spots with positions similar to UER, UGP, and UGD were clearly recognized when the 2-DE images of Li *et al.* (18) were examined. In-depth biochemical and physiological studies indicated that the rate of pectin biosynthesis, not general cell wall polysaccharide biosynthesis, may play a key role in sustaining the fast and exaggerated fiber elongation because only pectin precursors promoted fiber growth in cultured cotton ovules.

Two previous cotton fiber proteomes (18, 40) identified proteins by searching the database against known polypeptides or ESTs in all plant species or other organisms. Another group used a locally constructed 376,100 *Gossypium* EST database to search for cotton polypeptides (39). However, even this group did not produce full-length cotton cDNAs to reconfirm the identified proteins, whereas all the currently identified proteins, except for α-1,4-glucan phosphorylase (spot 22), were confirmed by putative full-length cotton cDNAs (Table I). As shown in supplemental Table 4, no significant qualitative difference was observed when comparing the current proteome with that reported by Yang *et al.* (40) and Zhao *et al.* (39), who both used a modified protein extraction protocol (41). The *Ligon lintless* (Li_1) mutant and the *fl* mutant were used by Zhao *et al.* (39) and in the current work, respectively, to elucidate fiber growth mechanisms. Li_1 produces extremely shortened lint fibers of 6 mm in final lengths compared with 30 mm generally produced from wild type. Fibers on Li_1 ovules grow normally for ~5–7 days and are terminated around 13 dpa. Zhao *et al.* (39) suggested that the fiber elongation defect of this mutant might constitute a unique feature to fish out proteins important for this process. However, fiber growth in Li_1 is not null, and mechanisms controlling cell elongation, such as the ones discovered here by using the *fl* mutant, are likely actively operating early in the development. This may obscure the detection of key components regulating fiber elongation through a proteomics approach.

UDP-Rha is used for the synthesis of plant cell wall pectic polysaccharides and of some glycoproteins (42). Matrix polysaccharides (mainly pectins and hemicelluloses) are important constituents in the cell walls of developing fibers that may account for 30–50% of the total sugar content in these cells but decrease to less than 3% in the secondary cell wall thickening stage (43). Five functional copies of the UDP-glucose 4-epimerase (UGE) genes that synthesize UDP-Gal from UDP-Glc are found in the *Arabidopsis* genome. Genetic and biochemical studies showed that single mutants, such as *uge4*, and multiple mutants, such as *uge2,4*, *uge1,4*, and *uge1,2,4*, develop very short roots, whereas other double or

triple mutants displayed stunted morphology due to a failure in cell wall polymer biosynthesis (44, 45). Experimental data obtained by studying a different set of *UGEs* involved in the synthesis of D-Gal, termed *REB1/RHD1* for *root epidermal bulger 1* or *root hair defective 1*, revealed that galactosylation of xyloglucan, a different primary cell wall polymer, is required for some types of cell expansion (46, 47). Evidence has also been produced for at least some of the galacturonosyltransferases (GAUTs), which transfer GalA from UDP-GalA to the pectic polysaccharide homogalacturonan, to play a role in seed mucilage expansions (36). A mutation in the *Arabidopsis* Rab GTPase *RABA4D* disrupts normal pollen tube growth by altering the pattern of pectin deposition so that it is no longer present exclusively in its growing tip (48). These data suggest that the biosynthesis of nucleotide sugars is important for certain types of cell growth, such as the rapid linear elongation found in cotton fiber, *Arabidopsis* root hairs, and pollen tubes.

Sucrose synthase (Sus; EC 2.4.1.13) is encoded by one of the earliest up-regulated cotton genes during fiber initiation and elongation (49, 50). *Sus* is preferentially expressed in elongating fiber cells, but not in adjacent normal epidermal cells, and it is induced significantly upon exogenous ethylene treatment (7). Antisense suppression of *Sus* expression results in reduced hexose levels and osmotic potential in ovules of transgenic plants, leading to a fiberless phenotype (50). These authors proposed that suppression of *Sus* expression impairs the fiber cell wall integrity by reducing the supply of UDP-Glc essential for the synthesis of cellulose and many non-cellulose cell wall components (50). However, cellulose biosynthesis, which uses UDP-Glc as the primary substrate, is very slow in the early phases of fiber development, and the amount of cellulose increases only after the onset of the secondary wall synthesis around 15–20 dpa (3, 51). Therefore, biosynthesis of pectin precursors, which is activated early in the development (Fig. 1), may be responsible for utilizing the large amounts of UDP-Glc initially produced by Sus throughout the primary cell wall synthesis and fiber elongation stages. Cellulose biosynthesis may cut in at the end of the primary cell wall extension period to utilize the UDP-Glc continuously produced by Sus and UGP for secondary cell wall biosynthesis and deposition.

Recent literature indicate that ethylene may act as a positive regulator for cotton fiber cell elongation as well as for *Arabidopsis* root hair, apical hook, and hypocotyl development (7, 33, 52, 54, 55). *Arabidopsis* mutants deficient in ethylene responses have significantly shorter root hairs, whereas exogenous application of the ethylene precursor 1-aminocyclopropane-1-carboxylic acid results in longer or ectopic root hairs (56, 57). Ethylene regulates *Rumex palustris* petiole elongation by modulating the expression of the cell wall protein *EXP1* (58). In arrowhead tubers (*Sagittaria pygmaea*), ethylene enhances the accumulation of transcripts encoding the hemicellulose modification protein endotransglucosylase hydrolase (SpXTH1) after 12 h of incubation with a stimulatory effect on shoot elongation under ambient air or 1% O_2 conditions (59). Exogenous ethylene was used to restore the biosynthesis of galactose-containing xyloglucan and arabinosylated galactan cell wall polymers back to wild-type levels in the *Arabidopsis rhd1* mutant, which produces no root hair due to the loss of a functional *UGE4* gene (53). Taken together with our results, we conclude that ethylene participates in the regulation of specific types of cell growth by activating genes involved in cell wall polymer biosynthesis, metabolism, or transport.

Acknowledgments—We thank Drs. Xiao-Ya Chen and Xue-Bao Li for contributing to the 31,401 cotton UniESTs. We are grateful to Dr. Hongbin Li of Shi-He-Zi University for preparing the spectra of cotton fiber proteins.

* This work was supported by China National Basic Research Program Grant 2004CB117302, National Natural Science Foundation of China Grant 90717009, the 111 project from the Chinese Ministry of Education, and a Natural Sciences and Engineering Research Council of Canada discovery grant (to T. L. W.).

S This article contains supplemental Tables 1–4, Figs. 1–9, and Spectra 1 and 2.

¶ Both authors contributed equally to this work.

** To whom correspondence may be addressed. E-mail: yu@cricaas.com.cn.

¶¶ To whom correspondence may be addressed: College of Life Sciences, Rm. E221, Peking University, Beijing 100871, China. Tel.: 86-10-62751193; Fax: 86-10-62754427; E-mail: zhuyx@water.pku.edu.cn.

REFERENCES

1. John, M. E., and Keller, G. (1996) Metabolic pathway engineering in cotton: biosynthesis of polyhydroxybutyrate in fiber cells. *Proc. Natl. Acad. Sci. U.S.A.* **93,** 12768–12773
2. Ji, S., Lu, Y., Li, J., Wei, G., Liang X., and Zhu, Y. (2002) A β-tubulin-like cDNA expressed specifically in elongating cotton fibers induces longitudinal growth of fission yeast. *Biochem. Biophys. Res. Commun.* **296,** 1245–1250
3. Ji, S. J., Lu, Y. C., Feng, J. X., Wei, G., Li, J., Shi, Y. H., Fu, Q., Liu, D., Luo, J. C., and Zhu, Y. X. (2003) Isolation and analyses of gene preferentially expressed during early cotton fiber development by subtractive PCR and cDNA array. *Nucleic Acids Res.* **31,** 2534–2543
4. Kim, H. J., and Triplett, B. A. (2001) Cotton fiber growth *in planta* and *in vitro.* Models for plant cell elongation and cell wall biogenesis. *Plant Physiol.* **127,** 1361–1366
5. Wilkins, T. A., and Arpat, A. B. (2005) The cotton fiber transcriptome. *Physiol. Plant.* **124,** 295–300
6. Singh, B., Avci, U., EichlerInwood, S. E., Grimson, M. J., Landgraf, J., Mohnen, D., Sørensen, I., Wilkerson, C. G., Willats, W. G., and Haigler, C. H. (2009) A specialized outer layer of the primary cell wall joins elongating cotton fibers into tissue-like bundles. *Plant Physiol.* **150,** 684–699
7. Shi, Y. H., Zhu, S. W., Mao, X. Z., Feng, J. X., Qin, Y. M., Zhang, L., Cheng, J., Wei, L. P., Wang, Z. Y., and Zhu, Y. X. (2006) Transcriptome profiling, molecular biological, and physiological studies reveal a major role for ethylene in cotton fiber cell elongation. *Plant Cell* **18,** 651–664
8. Xu, Y., Li, H. B., and Zhu, Y. X. (2007) Molecular biological and biochemical studies reveal new pathways important for cotton fiber development. *J. Integr. Plant Biol.* **49,** 69–74
9. Qin, Y. M., Pujol, F. M., Shi, Y. H., Feng, J. X., Liu, Y. M., Kastaniotis, A. J., Hiltunen, J. K., and Zhu, Y. X. (2005) Cloning and functional characterization of two cDNAs encoding NADPH-dependent 3-ketoacyl-CoA reductase from developing cotton fibers. *Cell Res.* **15,** 465–473
10. Gou, J. Y., Wang, L. J., Chen, S. P., Hu, W. L., and Chen, X. Y. (2007) Gene

expression and metabolite profiles of cotton fiber during cell elongation and secondary cell wall synthesis. *Cell Res.* **17,** 422–434
11. Song, W. Q., Qin, Y. M., Saito, M., Shirai, T., Pujol, F. M., Kastaniotis, A. J., Hiltunen, J. K., and Zhu, Y. X. (2009) Characterization of two cotton cDNAs encoding trans-2-enoyl-CoA reductase reveals a putative novel NADPH-binding motif. *J Exp. Bot.* **60,** 1839–1848
12. Qin, Y. M., Hu, C. Y., Pang, Y., Kastaniotis, A. J., Hiltunen, J. K., and Zhu, Y. X. (2007) Saturated very-long-chain fatty acids promote cotton fiber and *Arabidopsis* cell elongation by activating ethylene biosynthesis. *Plant Cell* **19,** 3692–3704
13. Tang, W., Deng, Z., Oses-Prieto, J. A., Suzuki, N., Zhu, S., Zhang, X., Burlingame, A. L., and Wang, Z. Y. (2008) Proteomics studies of brassinosteroid signal transduction using prefractionation and two-dimensional DIGE. *Mol. Cell. Proteomics* **7,** 728–738
14. Wienkoop, S., Morgenthal, K., Wolschin, F., Scholz, M., Selbig, J., and Weckwerth, W. (2008) Integration of metabolomic and proteomic phenotypes: analysis of data covariance dissects starch and RFO metabolism from low and high temperature compensation response in *Arabidopsis thaliana*. *Mol. Cell. Proteomics* **7,** 1725–1736
15. Choudhary, M. K., Basu, D., Datta, A., Chakraborty, N., and Chakraborty, S. (2009) Dehydration-responsive nuclear proteome of rice (*Oryza sativa* L.) illustrates protein network, novel regulators of cellular adaptation, and evolutionary perspective. *Mol. Cell. Proteomics* **8,** 1579–1598
16. Zhang, T., and Pan, J. (1992) Genetic analysis of a fuzzless-lintless mutant in *Gossypium hirsutum* L. *Jiangsu J. Agric. Sci.* **7,** 13–16
17. Feng, J. X., Liu, D., Pan, Y., Gong, W., Ma, L. G., Luo, J. C., Deng, X. W., and Zhu, Y. X. (2005) An annotation update via cDNA sequence analysis and comprehensive profiling of developmental, hormonal or environmental responsiveness of the Arabidopsis AP2/EREBP transcription factor gene family. *Plant Mol. Biol.* **59,** 853–868
18. Li, H. B., Qin, Y. M., Pang, Y., Song, W. Q., Mei, W. Q., and Zhu, Y. X. (2007) A cotton ascorbate peroxidase is involved in hydrogen peroxide homeostasis during fibre cell development. *New Phytol.* **175,** 462–471
19. Fu, Q., Wang, B. C., Jin, X., Li, H. B., Han, P., Wei, K. H., Zhang, X. M., and Zhu, Y. X. (2005) Proteomic analysis and extensive protein identification from dry, germinating *Arabidopsis* seeds and young seedlings. *J. Biochem. Mol. Biol.* **38,** 650–660
20. Wang, B. C., Wang, H. X., Feng, J. X., Meng, D. Z., Qu, L. J., and Zhu, Y. X. (2006) Post-translational modifications, but not transcriptional regulation, of major chloroplast RNA-binding proteins are related to *Arabidopsis* seedling development. *Proteomics* **6,** 2555–2563
21. Zulak, K. G., Khan, M. F., Alcantara, J., Schriemer, D. C., and Facchini, P. J. (2009) Plant defense responses in opium poppy cell cultures revealed by liquid chromatography-tandem mass spectrometry proteomics. *Mol. Cell. Proteomics* **8,** 86–98
22. Liu, Y., He, J., Ji, S., Wang, Q., Pu, H., Jiang, T., Meng, L., Yang, X., and Ji, J. (2008) Comparative studies of early liver dysfunction in senescence-accelerated mouse using mitochondrial proteomics approaches. *Mol. Cell. Proteomics* **7,** 1737–1747
23. Majeran, W., Zybailov, B., Ytterberg, A. J., Dunsmore, J., Sun, Q., and van Wijk, K. J. (2008) Consequences of C_4 differentiation for chloroplast membrane proteomes in maize mesophyll and bundle sheath cells. *Mol. Cell. Proteomics* **7,** 1609–1638
24. Huang, X., and Madan, A. (1999) CAP3: A DNA sequence assembly program. *Genome Res.* **9,** 868–877
25. Wan, C. Y., and Wilkins, T. A. (1994) A modified hot borate method significantly enhances the yield of high-quality RNA from cotton (*Gossypium hirsutum* L.). *Anal. Biochem.* **223,** 7–12
26. Mao, X., Cai, T., Olyarchuk, J. G., and Wei, L. (2005) Automated genome annotation and pathway identification using the KEGG orthology (KO) as a controlled vocabulary. *Bioinformatics* **21,** 3787–3793
27. Han, P., Li, Q., and Zhu, Y. X. (2008) Mutation of Arabidopsis *BARD1* causes meristem defects by failing to confine *WUSCHEL* expression to the organizing center. *Plant Cell* **20,** 1482–1493
28. Updegraff, D. M. (1969) Semimicro determination of cellulose in biological materials. *Anal. Biochem.* **32,** 420–424
29. Usadel, B., Kuschinsky, A. M., Rosso, M. G., Eckermann, N., and Pauly, M. (2004) RHM2 is involved in mucilage pectin synthesis and is required for development of the seed coat in *Arabidopsis*. *Plant Physiol.* **134,** 286–295
30. Western, T. L., Young, D. S., Dean, G. H., Tan, W. L., Samuels, A. L., and Haughn, G. W. (2004) MUCILAGE-MODIFIED4 encodes a putative pectin biosynthetic enzyme developmentally regulated by *APETALA2*, *TRANSPARENT TESTA GLABRA1*, and *GLABRA2* in the *Arabidopsis* seed coat. *Plant Physiol.* **134,** 296–306
31. Oka, T., Nemoto, T., and Jigami, Y. (2007) Functional analysis of *Arabidopsis thaliana* RHM2/MUM4, a multidomain protein involved in UDP-D-glucose to UDP-L-rhamnose conversion. *J. Biol. Chem.* **282,** 5389–5403
32. Kochanowski, N., Blanchard, F., Cacan, R., Chirat, F., Guedon, E., Marc, A., and Goergen, J. L. (2006) Intracellular nucleotide and nucleoside sugar contents of cultured CHO cells determined by as fast, sensitive, and high-resolution ion-pair RP-HPLC. *Anal. Biochem.* **348,** 243–251
33. Cho, H. T., and Cosgrove, D. J. (2002) Regulation of root hair initiation and expansin gene expression in *Arabidopsis*. *Plant Cell* **14,** 3237–3253
34. Seifert, G. J. (2004) Nucleotide sugar interconversions and cell wall biosynthesis: how to bring the inside to the outside. *Curr. Opin. Plant Biol.* **7,** 277–284
35. Mølhøj, M., Verma, R., and Reiter, W. D. (2004) The biosynthesis of D-galacturonate in plants. Functional cloning and characterization of a membrane-anchored UDP-D-glucuronate 4-epimerase from Arabidopsis. *Plant Physiol.* **135,** 1221–1230
36. Caffall, K. H., Pattathil, S., Phillips, S. E., Hahn, M. G., and Mohnen, D. (2009) Arabidopsis thaliana T-DNA mutants implicate *GAUT* genes in the biosynthesis of pectin and xylan in cell walls and seed testa. *Mol. Plant* **2,** 1000–1014
37. Alonso, J. M., Stepanova, A. N., Leisse, T. J., Kim, C. J., Chen, H., Shinn, P., Stevenson, D. K., Zimmerman, J., Barajas, P., Cheuk, R., Gadrinab, C., Heller, C., Jeske, A., Koesema, E., Meyers, C. C., Parker, H., Prednis, L., Ansari, Y., Choy, N., Deen, H., Geralt, M., Hazari, N., Hom, E., Karnes, M., Mulholland, C., Ndubaku, R., Schmidt, I., Guzman, P., Aguilar-Henonin, L., Schmid, M., Weigel, D., Carter, D. E., Marchand, T., Risseeuw, E., Brogden, D., Zeko, A., Crosby, W. L., Berry, C. C., and Ecker, J. R. (2003) Genome-wide insertional mutagenesis of *Arabidopsis thaliana*. *Science* **301,** 653–657
38. Millar, A. A., Clemens, S., Zachgo, S., Giblin, E. M., Taylor, D. C., and Kunst, L. (1999) CUT1, an *Arabidopsis* gene required for cuticular wax biosynthesis and pollen fertility, encodes a very-long-chain fatty acid condensing enzyme. *Plant Cell* **11,** 825–838
39. Zhao, P. M., Wang, L. L., Han, L. B., Wang, J., Yao, Y., Wang, H. Y., Du, X. M., Luo, Y. M., and Xia, G. X. (2010) Proteomic identification of differentially expressed proteins in the *ligon lintless* mutant of upland cotton (*Gossypium hirsutum* L.). *J. Proteome Res.* **9,** 1076–1087
40. Yang, Y. W., Bian, S. M., Yao, Y., and Liu, J. Y. (2008) Comparative proteomic analysis provides new insights into the fiber elongating process in cotton. *J. Proteome Res.* **7,** 4623–4637
41. Yao, Y., Yang, Y. W., and Liu, J. Y. (2006) An efficient protein preparation for proteomic analysis of developing cotton fibers by 2-DE. *Electrophoresis* **27,** 4559–4569
42. Ridley, B. L., O'Neill, M. A., and Mohnen, D. (2001) Pectins: structure, biosynthesis, and oligogalacturonide-related signaling. *Phytochemistry* **57,** 929–967
43. Tokumoto, H., Wakabayashi, K., Kamisaka, S., and Hoson, T. (2002) Changes in the sugar composition and molecular mass distribution of matrix polysaccharides during cotton fiber development. *Plant Cell Physiol.* **43,** 411–418
44. Barber, C., Rösti, J., Rawat, A., Findlay, K., Roberts, K., and Seifert, G. J. (2006) Distinct properties of the five UDP-D-glucose/UDP-D-galactose 4-epimerase isoforms of *Arabidopsis thaliana*. *J. Biol. Chem.* **281,** 17276–17285
45. Rösti, J., Barton, C. J., Albrecht, S., Dupree, P., Pauly, M., Findlay, K., Roberts, K., and Seifert, G. J. (2007) UDP-glucose 4-epimerase isoforms UGE2 and UGE4 cooperate in providing UDP-galactose for cell wall biosynthesis and growth of *Arabidopsis thaliana*. *Plant Cell* **19,** 1565–1579
46. Nguema-Ona, E., Andème-Onzighi, C., Aboughe-Angone, S., Bardor, M., Ishii, T., Lerouge, P., and Driouich, A. (2006) The *reb1-1* mutation of Arabidopsis. Effect on the structure and localization of galactose-containing cell wall polysaccharides. *Plant Physiol.* **140,** 1406–1417
47. Wubben, M. J., 2nd, Rodermel, S. R., and Baum, T. J. (2004) Mutation of a UDP-glucose-4-epimerase alters nematode susceptibility and ethylene responses in Arabidopsis roots. *Plant J.* **40,** 712–724
48. Szumlanski, A. L., and Nielsen, E. (2009) The Rab GTPase RabA4d regu-

lates pollen tube tip growth in *Arabidopsis thaliana. Plant Cell* **21,** 526–544
49. Ruan, Y. L., and Chourey, P. S. (1998) A fiberless seed mutation in cotton is associated with lack of fiber cell initiation in ovule epidermis and alterations in sucrose synthase expression and carbon partitioning in developing seeds. *Plant Physiol.* **118,** 399–406
50. Ruan, Y. L., Llewellyn, D. J., and Furbank, R. T. (2003) Suppression of sucrose synthase gene expression represses cotton fiber cell initiation, elongation, and seed development. *Plant Cell* **15,** 952–964
51. Haigler, C. H., Zhang, D. S., and Wilkerson, C. G. (2005) Biotechnological improvement of cotton fiber maturity. *Physiol. Plant.* **124,** 285–294
52. Achard, P., Vriezen, W. H., Van Der Straeten, D., and Harberd, N. P. (2003) Ethylene regulates Arabidopsis development via the modulation of DELLA protein growth repressor function. *Plant Cell* **15,** 2816–2825
53. Seifert, G. J., Barber, C., Wells, B., and Roberts, K. (2004) Growth regulators and the control of nucleotide sugar flux. *Plant Cell* **16,** 723–730
54. De Grauwe, L., Vandenbussche, F., Tietz, O., Palme, K., and Van Der Straeten, D. (2005) Auxin, ethylene and brassinosteroids: tripartite control of growth in the Arabidopsis hypocotyl. *Plant Cell Physiol.* **46,** 827–836
55. Stepanova, A. N., Hoyt, J. M., Hamilton, A. A., and Alonso, J. M. (2005) A link between ethylene and auxin uncovered by the characterization of two root-specific ethylene-insensitive mutants in *Arabidopsis. Plant Cell* **17,** 2230–2242
56. Pitts, R. J., Cernac, A., and Estelle, M. (1998) Auxin and ethylene promote root hair elongation in *Arabidopsis. Plant J.* **16,** 553–560
57. Tanimoto, M., Roberts, K., and Dolan, L. (1995) Ethylene is a positive regulator of root hair development in *Arabidopsis thaliana. Plant J.* **8,** 943–948
58. Vreeburg, R. A., Benschop, J. J., Peeters, A. J., Colmer, T. D., Ammerlaan, A. H., Staal, M., Elzenga, T. M., Staals, R. H., Darley, C. P., McQueen-Mason, S. J., and Voesenek, L. A. (2005) Ethylene regulates fast apoplastic acidification and expansin A transcription during submergence-induced petiole elongation in *Rumex palustris. Plant J.* **43,** 597–610
59. Ookawara, R., Satoh, S., Yoshioka, T., and Ishizawa, K. (2005) Expression of α-expansin and xyloglucan endotransglucosylase/hydrolase genes associated with shoot elongation enhanced by anoxia, ethylene and carbon dioxide in arrowhead (*Sagittaria pygmaea* Miq.) tubers. *Ann. Bot.* **96,** 693–702